

# Pharmacophore Modeling, Docking Studies, and Synthesis of Novel Dipeptide Proteasome Inhibitors Containing Boron Atoms

Meng Lei,<sup>†</sup> Xin Zhao,<sup>‡</sup> Zhanli Wang,<sup>\*,§</sup> and Yongqiang Zhu<sup>\*,‡</sup>

College of Science, Nanjing Forestry University, No. 159 Longpan Road, Nanjing 210037, PRC, Jiangsu Simcere Pharmaceutical Research Institute and Jiangsu Key Laboratory of Molecular Targeted Antitumor Drug Research, No. 699-18 Xuan Wu Avenue, Xuan Wu District, Nanjing 210042, PRC, and Technology Center, NeoTrident Technology Ltd., No. 620 Zhangyang Road, Pudong District, Shanghai 200122, PRC

Received June 26, 2009

A 3D pharmacophore model had been generated for a series of dipeptide proteasome inhibitors containing boron atoms using Catalyst. A data set consisting of 24 inhibitors was selected on the basis of the information content of the structures and activity data as required by the Catalyst/HypoGen program. The built model was able to predict the activity of other known proteasome inhibitors not included in the model generation. Based on the analysis of the best hypotheses, some novel proteasome inhibitors were designed and predicted. Three dipeptide boronic acid inhibitors **SMNT 1**, **SMNT 2**, and **SMNT 3**, were synthesized and biologically assayed. It turned out that the three designed molecules were all more potent than the marketed **MG341**, and the experimental values were consistent with the predicted ones, indicating that the theoretical model was reliable enough to predict and design novel proteasome inhibitors. The covalent interaction mode between the boron atom of the inhibitor and O<sup>γ</sup>-Thr1 residue of the 20S proteasome was studied for the first time by employing the most potent inhibitor **SMNT 2** with the Insight II 2005/Affinity program. The docking results agreed well with the experimental ones.

## INTRODUCTION

The ubiquitin-proteasome pathway (UPP) is very critical to the intracellular protein homeostasis.<sup>1</sup> Many important biological processes<sup>2–9</sup> such as cell cycle and cytokine-stimulated signal transduction are regulated by this pathway. The proteasome is a validated target for treatment of cancers since the FDA has approved the first proteasome inhibitor bortezomib (MG341, or PS-341) for the therapy of multiple myeloma (MM) and mantle cell lymphoma (MCL) in 2003 and 2006, respectively. The proteasome consists of a multicatalytic protein core particle (CP) known as the 20S proteasome and the regulatory particles (RPs) known as the 19S proteasome. The RPs are responsible for the recognition of ubiquitinated proteins and then unfold and translocate them into the CP cavity where the protein degradation takes place. The CP is composed of four stacks arranged as ( $\alpha_1\text{-}\alpha_7$ ,  $\beta_1\text{-}\beta_7$ )<sub>2</sub>, of which the  $\beta_1$ ,  $\beta_2$ , and  $\beta_5$  subunits have the chymotrypsin-like (CT-L), trypsin-like (T-L), and post-glutamyl peptide hydrolysis (PGPH) activities. Each subunit utilizes the hydrophilic  $\gamma$ -hydroxyl group of the *N*-terminal threonine (Thr) to hydrolyze the amide bond of protein substrate.

Previously, the proteasome inhibitors, acting as a useful tool, greatly contributed to the investigation of many important cellular processes regulated by the UPP. However,

nowadays, many structural diversity proteasome inhibitors not only were used as research tools and but also some of them entered the clinical trials. It is worthy to note a dipeptide boronic acid, bortezomib, which was approved by the FDA in May 2003, the EMEA in April 2004, and Japan in October 2006, respectively, for the treatment of multiple myeloma (MM) patients who have received one prior therapy but failed.<sup>10</sup> On December 8, 2006, the FDA granted full approval of bortezomib for the treatment of patients with relapsed mantle cell lymphoma (MCL). And now it is also under investigation in phase I, phase II, and phase III studies for a wide variety of hematological malignancies and solid tumors, including non-Hodgkin's lymphoma, prostate, breast, and nonsmall cell lung cancers.<sup>11–13</sup> In 2005, this drug won the 'Prix Galien' award in Belgium, Netherland, and France, which is considered the highest accolade for pharmaceutical R&D - the industry equivalent of Nobel Prize. At the same time, this drug set the milestone of the development of proteasome inhibitors: among all the proteasome inhibitors, it was first marketed and was also the first marketed peptide compound containing boron atom. Dipeptide boronic acid analogs covalently inhibit the proteasome by reacting with the hydroxyl group of the *N*-terminal threonines of the  $\beta$  subunits to form a reversible tetrahedral adduct, which has been confirmed by X-ray diffraction of complex of MG341-20S proteasome.<sup>14</sup> Peptide boronates are much more selective due to their weaker interactions with thiol proteases and serine proteases compared with other proteasome inhibitors, such as peptide aldehyde.<sup>15</sup> However, recent clinical trials reported some adverse events of bortezomib, including peripheral neuropathy, hypotension, neutropenia, thromb-

\* Corresponding author phone: 86-21-58353866; fax: 86-21-58356260; e-mail: wang.zhanli@hotmail.com (Z.L.); phone: 86-25-85566666-1726; fax: 86-21-85566666-1835; e-mail: zhyqscu@hotmail.com (Y.Q.).

<sup>†</sup> Nanjing Forestry University.

<sup>‡</sup> Jiangsu Simcere Pharmaceutical Research Institute and Jiangsu Key Laboratory of Molecular Targeted Antitumor Drug Research.

<sup>§</sup> NeoTrident Technology Ltd.

ocytopenia, etc.<sup>16</sup> So the development of such kind of drug is focused on how to design more potent and specific inhibitors.

Chemical feature based pharmacophore model may serve as a guide in the design of more selective inhibitors. Though many different peptide boronate inhibitors had been synthesized and experimentally assessed, to the best of our knowledge, there is no information available regarding pharmacophore for such kind of compounds up to date. As a continuation of our effort to design and discover more potent and specific proteasome inhibitors,<sup>17–19</sup> this study aims to construct the chemical feature based pharmacophore models for dipeptide boronic acid proteasome inhibitors. The models were validated and finally used in designing new leads for hopefully more active compounds. At the same time, we reported the covalent binding mode of the most active compound with the 20S proteasome using docking method for the first time.

## RESULTS AND DISCUSSION

Continuing our investigation in this field and in an attempt to identify novel proteasome inhibitors, 3D pharmacophore models for proteasome inhibitors were constructed using a training set. The best hypothesis has quantitatively predictive ability in terms of activity and then was used to guide the rational design of novel dipeptide boronic acid as potent proteasome inhibitors.

**Generation and Evaluation of the Hypothesis.** This study was performed using the software package Catalyst<sup>20</sup> installed on an Silicon Graphic O2 workstation. A set of boronic acid analogues<sup>21</sup> was used as the training set to generate pharmacophore models (Table 1). To ensure the statistic relevance of the calculated model, the training set contained 24 compounds together with their activity values and the range of in vitro proteasome binding activity ( $K_i$  value) spanned 5 orders of magnitude (0.03–2300 nM). Hydrogen bond acceptor (HBA), hydrogen bond donor (HBD), hydrophobic (HY), ring aromatic, and positive ionizable (PI) were selected to form the essential information. It had been shown that the boronic acid group was covalently bound to the O<sup>γ</sup>-Thr1 residue of the 20S proteasome<sup>14</sup> and is very critical for proteasome inhibitory activity. However, it does not satisfy the positive ionizable function of boron atoms provided within Catalyst by default. Thus, we added this feature by applying the Exclude/Or Quick Tool to make the program recognize the boron atoms as positive ionizable function.

Based on the training set, ten hypotheses were constructed according to their ranking scores by the algorithm HypoGen (Table 2). All 10 hypotheses contained the same features, HBA, HBD, PI, and two HYs. These features are therefore assumed to be necessary for the proteasome inhibitory activity.

The output parameters determine the quality of hypotheses. Hypotheses are believed to be statistically relevant when the total hypothesis cost is close to the fixed and far away from null cost values. In our results, the cost difference between the Null Hypothesis (218.463) and the Fixed Cost (92.627) amount to 125.836, which is much higher than 70. Moreover, the configuration cost is 10.776, which is less than 17. These results indicate a reliable ability of the generated pharma-

cophore models to predict training set compounds activities and confirm that it did not come about by chance.

The CatScramble program within Catalyst was applied to further evaluate the statistical relevance of the model. The experimental activities in the training set were scrambled randomly, and the resulting training set was used for a HypoGen run. Thereby all parameters were adopted from the initial HypoGen calculation. This procedure was reiterated 19 times. The output file of Catalyst run (see the Supporting Information, SI) listed the randomized data. This result indicates that there is a 95% chance for model to represent a true correlation in the training set activity data.

The first hypothesis (Hypo1) was characterized by the highest cost difference (79.755), lowest rms error (1.86507), and the best correlation coefficient (0.837464). As mentioned before, due to the fact that the Total Cost of the best hypothesis is much closer to the Fixed Cost than the Null Cost, Hypo1 had a reliable ability to predict the activities of training set compounds. Thus, Hypo1 was selected for further analysis. Figure 1a shows the mapping of the most active compounds **MG329** in the training set on the Hypo1. As expected, PI involved the boronic acid group, while HBA and HBD involved respectively the carbonyl group and nitrogen atom, and two HY functions mapped well with hydrophobic naphthyl and cyclohexyl ring.

We further used a test set of 26 molecules (Table 3), including the recently marketed **MG341**, to validate model Hypo1. Hypo1 was regressed against the compounds of the test set, and a score of 0.873 was achieved. Among the 26 molecules in the test set, 23 values were predicted with error factors less than 10. The 3 remaining estimations were carried out with error factors below 30. The average of the error factors for the test set was 4.312. In summary, it could be confirmed that the validity of the Hypo1 in predicting the activities of proteasome inhibitors with different structural classes, which were not included in the training set.

**Rational Design of New Dipeptide Boronic Acids as Proteasome Inhibitors.** The main purpose of our work is to identify new lead structures. Therefore, Hypo1 was used to guide the rational design of novel dipeptide boronic acids as potent proteasome inhibitors. Generally, more active molecules map well to all the features of the hypothesis, and compounds showing low activities map poorly to the hypothesis. Among the five features of the Hypo1, most of the less active compounds such as **MG337**, **MG339**, **MG347**, and **MG359** were unable to map the Hy2 feature, as shown by the presence of an asterisk in the mapping column of the output file of Catalyst run (see SI).

**MG341** is a recently marketed drug and was mapped to Hypo1 (Figure 1b). The estimated activity (0.54 nM) of **MG341** is similar to the measured one (0.6 nM) with a relative error of −0.1. Furthermore, the conformation of the crystal structure of **MG341** was compared with that of the optimized one generated by Catalyst. A remarkable similarity was observed between these two conformations (rmsd: 2.892 Å) (Figure 2). This result is a significant confirmation for the alignment reliability between the Hypo1 and **MG341**.

It is worth noting that the marketed compound **MG341** did not map the Hy1 feature quite well, and we speculate that the proteasome inhibitory potency might be improved by introduction of functionality in this ligand, which might map to the Hy1 feature of the Hypo1. Thus, the pyrazine

**Table 1.** Training Set and *Ki* Values Used in the Generation of the Pharmacophore for Proteasome Inhibitors

compd	P <sup>1</sup>	P <sup>2</sup>	P <sup>3</sup>	<i>Ki</i> (nM)	compd	P <sup>1</sup>	P <sup>2</sup>	P <sup>3</sup>	<i>Ki</i> (nM)
MG264				119	MG310				90
MG267				0.1	MG313				42
MG270				0.083	MG323				850
MG274				3	MG328				0.088
MG284				1200	MG329				0.03
MG286				0.15	MG337				230
MG289				6.3	MG339				1600
MG291				0.28	MG344				51
MG293				2300	MG347				29
MG294	H			152	MG359				5.5
MG298				0.075	MG387				0.20
MG302	H			7.5					
MG305				189					

ring at the Hy1 function position of compound **MG341** was replaced with the hydrophobic 1-naphthyl group (**SMNT 1**). We then used Hypo1 to estimate **SMNT 1**, and it allowed proper mapping of the Hy1 feature of the generated hypothesis, and the predicted *Ki* value for **SMNT 1** was 0.22 nM. The mapping of **SMNT 1** onto the Hypo1 is represented in Figure 3a.

In fact, the Hy2 feature of Hypo1 also drew our attention. Figure 3a indicated that Hy2 was not located at the centroid of the benzyl function group of **SMNT 1**. It means this compound was unable to map this feature well. Moreover, the most active compound **MG329** in the data set mapped onto the Hypo1, and the naphthyl group overlaps neatly with the Hy2. Based on the above-mentioned observation, we

**Table 2.** Ten Hypotheses Constructed by HypoGen

Hypo <sup>a</sup>	total cost	cost diff <sup>b</sup>	rms	correl (r)	features <sup>c</sup>
Hypo1	138.708	79.755	1.86507	0.837464	HBA, HBD, HY, HY, PI
Hypo2	140.970	77.493	1.98678	0.810413	HBA, HBD, HY, HY, PI
Hypo3	150.066	68.397	2.18392	0.764586	HBA, HBD, HY, HY, PI
Hypo4	155.109	63.354	2.26559	0.743995	HBA, HBD, HY, HY, PI
Hypo5	159.386	59.077	2.34461	0.722313	HBA, HBD, HY, HY, PI
Hypo6	159.567	58.896	2.36138	0.717084	HBA, HBD, HY, HY, PI
Hypo7	160.504	57.959	2.37828	0.712190	HBA, HBD, HY, HY, PI
Hypo8	160.873	57.590	2.38342	0.710728	HBA, HBD, HY, HY, PI
Hypo9	163.736	54.727	2.38884	0.711367	HBA, HBD, HY, HY, PI
Hypo10	166.615	51.848	2.47644	0.682662	HBA, HBD, HY, HY, PI

<sup>a</sup> Numbers for the hypothesis are consistent with the numeration as obtained by the hypothesis generation. <sup>b</sup> Difference between the Null hypothesis and the cost of each returned hypothesis. <sup>c</sup> HBA: hydrogen bond acceptor; HBD: hydrogen bond donor; HY: hydrophobic; PI: positive ionizable.

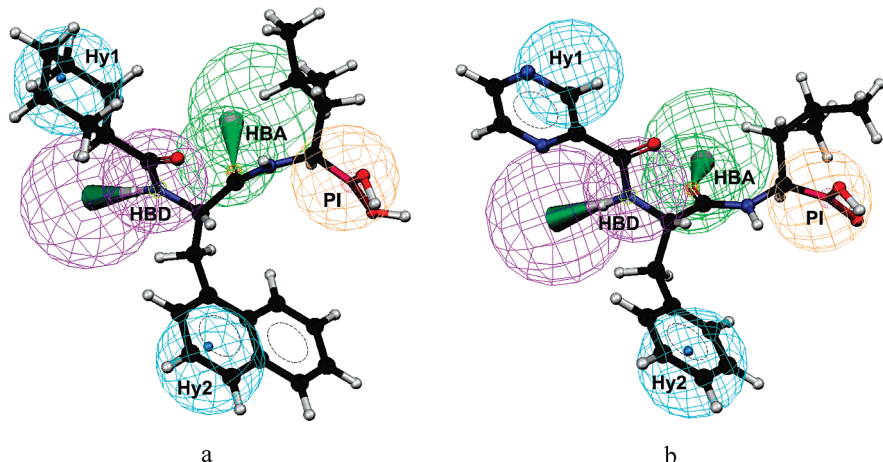


**Figure 1.** Best HypoGen pharmacophore model Hypo1 aligned to (a) the most active compound **MG329** in the training set and (b) marketed **MG341** in the test set.

thought that replacement of the phenyl group at the Hy2 function position by the 1-naphthyl group should provide enhanced proteasome inhibitory activity. So **SMNT 2** was designed and mapped onto the Hypo1 (Figure 3b). The predicted *Ki* value for **SMNT 2** was 0.13 nM, which was slightly more potent than **SMNT 1**. Based on the design of **SMNT 2**, we further investigated the predicted activity of the 2-naphthyl substituent at the Hy1 function position (**SMNT 3**) and mapped it onto the Hypo1 (Figure 3c), and the predicted *Ki* value for **SMNT 3** was 1.9 nM, and then synthesis and biological evaluation of the designed molecules were carried out to verify the calculated results. The experimental and predicted results were displayed in Table 4. It showed that the order of the biological activities of the designed molecules were consistent with that of theoretically calculated ones, that is **SMNT 2** > **SMNT 1** > **SMNT 3**. At the same time, the designed molecules were all more potent than the standard **MG341**, which indicated that the pharmacophore models built in this paper were powerful and reliable enough to design and predict novel proteasome inhibitors.

It was reported that the boron atom of **MG341** covalently interacted with the nucleophilic oxygen lone pair of the residue O<sup>γ</sup>-Thr1 of 20S proteasome.<sup>14</sup> However, calculation on the covalent bonds was always a challenging job so far, which greatly restricted the development of covalent inhibitors. Especially for peptidyl proteasome inhibitors containing boron atoms, no docking methods were reported so far. In order to attempt to set up a reliable theoretical method to

evaluate the O–B covalent bond and fully understand the interaction mode between the inhibitor and 20S proteasome, the highest active compound **SMNT 2** was selected for docking studies. The Affinity program within Insight II 2005 was used.<sup>22</sup> The consistent valence force field (CVFF) was selected prior to performing docking calculations. The active site β5 subunit was extracted from the crystal structure of the MG341-20S proteasome complex (PDB code: 2F16).<sup>14</sup> The initial position and conformation of **SMNT 2** were obtained by taking the crystal structure of **MG341** as the template. For the absence of the empirical potential energy function of the B atom in Insight II 2005, we adopted the same strategy reported in the literature<sup>23,24</sup> and changed the boron atom ‘B’ in **SMNT 2** to carbon atom ‘C.3’. Moreover, we retained only the 1094th water molecule at the receptor binding site for docking studies as it was found to stabilize the interaction of the ligand molecule.<sup>25</sup> Figure 4 showed the binding mode of **SMNT 2** in the proteasome binding site. We observed that hydrophobic interaction and hydrogen bond were the stabilizing force in this protein–ligand interaction, which was consistent with our previous results.<sup>18</sup> Hydrophobic groups were positioned in lipophilic pockets created by Ser20, Gln22, Pro24, and Ala27. The theoretical calculation indicated that compound **SMNT 2** formed hydrogen bonds with Thr1, Thr21, Gly47, Ala49, Ala50, and the 1094th water molecule, respectively, which were in agreement with the experimental results.<sup>14</sup> This docking results further confirmed that our pharmacophore models

**Table 3.** Test Set and *Ki* Values Used in the Generation of the Pharmacophore for Proteasome Inhibitors

compd	P <sup>1</sup>	P <sup>2</sup>	P <sup>3</sup>	Actual <i>Ki</i> (nM)	Estimated <i>Ki</i> (nM)	Error							
							compd	P <sup>1</sup>	P <sup>2</sup>	P <sup>3</sup>	Actual <i>Ki</i> (nM)	Estimated <i>Ki</i> (nM)	Error
MG273				0.18	0.5	2.8	MG340				480	290	-1.7
MG287				0.17	0.88	5.2	MG341				0.6	0.54	-1.1
MG290				5.4	2.6	-2.1	MG345				0.76	2	2.7
MG292				6.0	-1.7	-3.4	MG346				1.1	0.77	-1.4
MG299				0.14	1.8	13	MG349				18	30	1.7
MG301				1.3	1.2	-1.1	MG352				0.15	0.3	2
MG303	H-HCl			3.9	24	6.2	MG357				23	13	-1.7
MG306				0.23	0.72	3.1	MG363				3.45	19	5.5
MG316				22	28	1.3	MG364				1500	49	-30
MG319				20	12	-1.7	MG368				5.6	1.6	-3.5
MG322				2.2	1.2	-1.8	MG369				24.2	35	1.4
MG323				850	400	-2.1	MG385				23	7.2	-3.2
MG334				1.1	2.7	2.4	MG386				92	9.2	-10

were reasonable, and the docking method was reliable for the design of novel inhibitors.

The connolly molecular surface was then calculated using the Dephi module of the Insight II. The surface is color-coded by electrostatic potential as shown in Figure 5. The spectrum shows that negative and positive regions are opaque

red and blue, respectively. The electrostatic potential energy results showed that the center area was strongly positively (blue) and negatively charged (red) due to Arg and Glu residues surrounded by an area of neutral charge (white). Our results indicated that **SMNT 2** maintained the hydrophobic interaction as observed in the docking study.

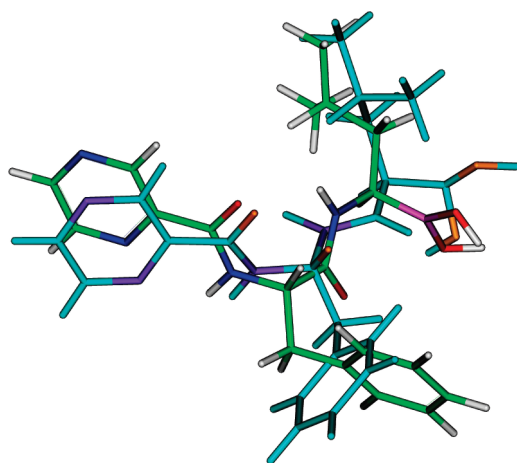


**Figure 2.** The conformation of the crystal structure of MG341 (light blue) was compared with that of the optimized one generated by Catalyst (green).

**Synthesis.** Scheme 1 summarized the synthesis of the target molecules **SMNT 1–3** and **MG341**. The key intermediate **3** was prepared according to the conventional liquid-phase synthesis.<sup>26</sup> (*S*)-Methyl ester amino acid hydrochlorides **1** was coupled with 1-naphthoic acid or 2-naphthoic acid in the presence of DCC and HOBT to give methyl esters **2**, which was not separated and directly used for saponification to afford acids **3** in high yield. Coupling of the known amino boronate **4** with various acids **3** in the presence of EDC•HCl and HOBT afforded the dipeptidyl boronates **5**, which was transesterified with isobutylboronic acid under acid conditions to give boronic acids **SMNT 1–3** and **MG341** in moderate yields after chromatographic purification.

**Table 4.** Structures of Compounds SMNT 1–3 and MG341 and Their Inhibition of Human 20S Proteasome

compd	P <sup>1</sup>	P <sup>2</sup>	IC <sub>50</sub> (obsd, nM) <sup>a</sup>	K <sub>i</sub> (calcd, nM) <sup>b</sup>
<b>SMNT 1</b>			0.41	0.22
<b>SMNT 2</b>			0.25	0.13
<b>SMNT 3</b>			0.95	1.90
<b>MG341</b>			1.02 <sup>c</sup>	0.54

<sup>a</sup> obsd, observed IC<sub>50</sub> values. <sup>b</sup> calcd, calculated K<sub>i</sub> values. <sup>c</sup> IC<sub>50</sub> value obtained for MG341 under our experimental conditions.

## CONCLUSIONS

In conclusion, a manually developed Catalyst pharmacophore had been validated with a series of dipeptide proteasome inhibitors containing boron atoms. The confirmed pharmacophore model was used to design some novel inhibitors. After synthesis and biological assay, it showed

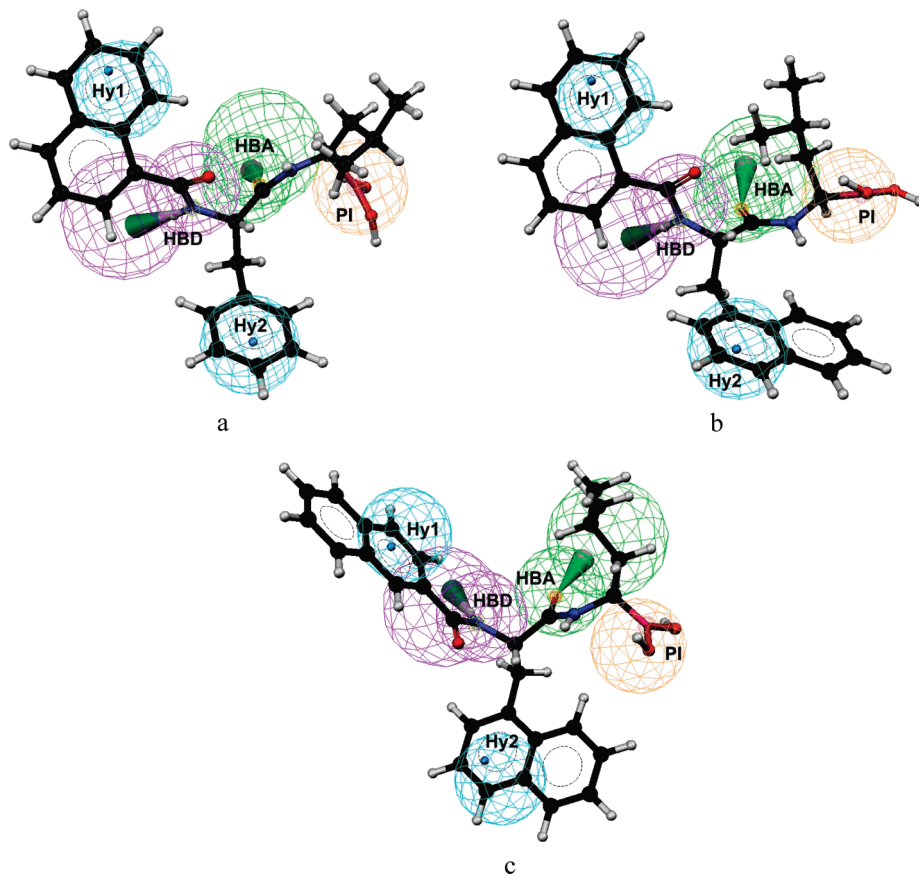


**Figure 3.** Hypol aligned to three designed molecules: (a) SMNT 1; (b) SMNT 2; and (c) SMNT 3.

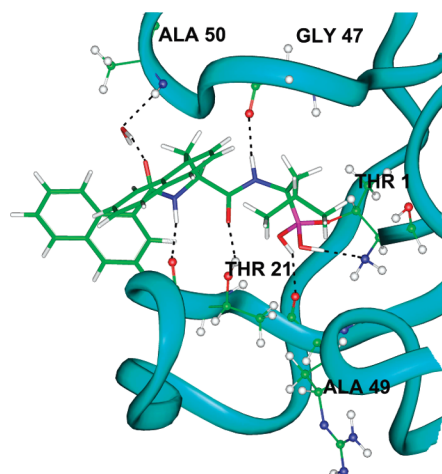


**Figure 4.** Binding of SMNT 2 to the active site of proteasome.

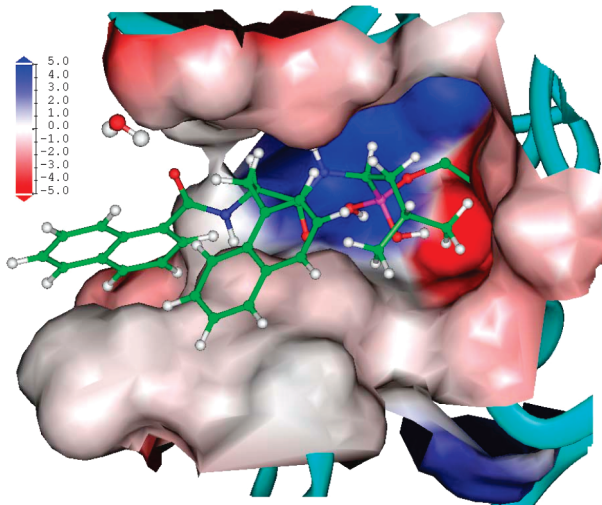


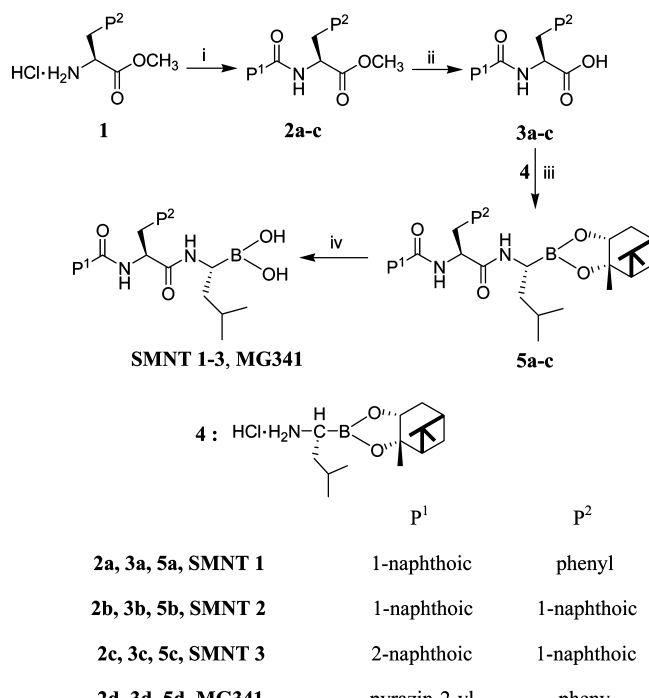
**Figure 5.** Proteasome active site model with SMNT 2 in the active site.

the three designed inhibitors inhibited the 20S proteasome at less than 1 nM, more potent than the drug **MG341** on the market. The experimental results suggested that the built 3D pharmacophore model was powerful to design the structurally novel proteasome inhibitors. We also presented for the first time the study of covalent binding mode between the boron atom of boronic acid inhibitors and the residue O<sup>γ</sup>-Thr1 of 20S proteasome using the docking method. The interaction mode between the most active **SMNT 2** and residues in the active site of 20S proteasome was similar to what had been observed in the **MG341**-20S proteasome crystal complex. This docking result further validated the robustness of the 3D pharmacophore.

## EXPERIMENTAL SECTION

**Chemistry.** Commercially available reagents were used directly without any purification unless otherwise stated. Absolutely anhydrous solvents were obtained with the proper methods introduced in the literature. Yields refer to chromatographically unless otherwise stated. Reactions were monitored by thin-layer chromatography carried out on silica gel aluminum sheets (60F-254) and RP-18 F254s using UV light as a visualizing agent and 15% ethanolic phosphomolybdic acid and heat or ninhydrin and heat as a developing

**Scheme 1.** General Synthesis of SMNT 1–3 and MG341<sup>a</sup>



<sup>a</sup> Reagents and conditions: (i) P<sup>1</sup>-COOH, DCC, HOBT, NMM, THF, 0 °C; (ii) (1) 2 N NaOH, acetone, 0 °C; (2) 2 N HCl, ethyl acetate, 0 °C. (iii) EDC·HCl, HOBT, DIPEA, CH<sub>2</sub>Cl<sub>2</sub>, –15 °C to room temp; (iv) isobutylboronic acid, 2 N HCl, MeOH, hexane.

agent. Column chromatography was performed on 200–300 mesh silica gel and ODS C-18 column. Analytical reverse phase HPLC was run using a Kromasil 100-5C18, 4.6 mm × 250 mm column eluting with a mixture of methanol and water containing 0.02% triethylamine and 0.03% trifluoroacetic acid. HPLC showed purity of all the final products was greater than 95%. Melting points were obtained on an YRT-3 melting point apparatus and were uncorrected. <sup>1</sup>H NMR and <sup>13</sup>C NMR spectra were recorded at room temperature on a Bruker Avance 300 or Avance 500 spectrometers. Chemical shifts were reported in ppm ( $\delta$  units), and tetramethylsilane (TMS) was used as internal reference. The following abbreviations were used to designate the multiplicities: s = singlet, d = doublet, t = triplet, m = multiplet, dd = doublet of doublets. Mass spectra were obtained using Agilent LC-MS (1956B) instruments in electrospray positive and negative ionization modes. High-resolution mass spectra were recorded on a ZAB-HS instrument using an electrospray source (ESI).

The synthesis of the target compounds was shown below. A typical procedure for preparation of dipeptide boronic acids **SMNT 1–3** was exemplified by the synthesis of **MG341**. For description of general methods and preparation of acids **3a-d**, see the SI.

**N-[(1S)-1-[[[(1R)-1-[(3aS,4S,6S,7aR)-Hexahydro-3a,5,5-trimethyl-4,6-methano-1,3,2-benzodioxaborol-2-yl]-3-methylbutyl]amino]carbonyl]-2-phenyl]-2-pyrazincarboxamide (5d).** To a cooled solution (–5 °C) of pyrazin-L-phenyl alanine **3a** (0.27 g, 1.00 mmol) dissolved in anhydrous CH<sub>2</sub>Cl<sub>2</sub> (50 mL) was added HOBT (0.16 g, 1.20 mmol). After 20 min, the temperature of the reaction system was cooled to –15 °C and EDC·HCl (0.19 g, 1.00 mmol) was added. Finally the precooled (0 °C) mixture of the known pinanediol

boronate amino hydrochloride **4** (0.30 g, 1.00 mmol) and DIPEA (0.26 mL, 1.48 mmol) in anhydrous  $\text{CH}_2\text{Cl}_2$  (10 mL) was poured. The mixture stirred at  $-15^\circ\text{C}$  for 1 h and at room temperature for 2 h and was finally quenched with water. The aqueous phase was extracted with  $\text{CH}_2\text{Cl}_2$  ( $3 \times 100$  mL). The combined organic phase was washed with 10% citric acid, 5%  $\text{NaHCO}_3$ , and brine, dried over anhydrous  $\text{Na}_2\text{SO}_4$ , filtered, and evaporated to provide a crude product. ODS column chromatography using acetonitrile/ $\text{H}_2\text{O}$  (3:1) afforded 0.43 g (79.0%) of **12** as a glassy solid.  $^1\text{H}$  NMR ( $\text{CDCl}_3$ , 500 MHz)  $\delta$  0.82–0.85 ( $-\text{CH}_3$ , m, 9H), 1.16–1.51 ( $-\text{CH}_3$ ,  $-\text{CH}_2$ ,  $-\text{CH}$ , m, 10H), 1.77–1.92 ( $-\text{CH}_2$ ,  $-\text{CH}$ , m, 2H), 1.95–2.04 ( $-\text{CH}$ , m, 1H), 2.16–2.21 ( $-\text{CH}_2$ , m, 1H), 2.29–2.35 ( $-\text{CH}_2$ , m, 1H), 3.12–3.26 ( $-\text{CH}_2$ ,  $-\text{CH}$ , m, 3H), 4.25–4.31 ( $-\text{CH}$ , m, 1H), 4.78–4.83 ( $-\text{CH}$ , m, 1H), 5.78–5.94 ( $-\text{CONH}$ , m, 1H), 7.19–7.31 ( $-\text{Ph}$ , m, 5H), 8.38 ( $-\text{CONH}$ , t,  $J = 8.9$  Hz, 1H), 8.52–8.54 ( $-\text{Pyz}$ , m, 1H), 8.74 ( $-\text{Pyz}$ , t,  $J = 1.6$  Hz, 1H), 9.34–9.35 ( $-\text{Pyz}$ , m, 1H).  $^{13}\text{C}$  NMR ( $\text{CDCl}_3$ , 125 MHz)  $\delta$  22.00, 22.84, 24.00, 25.48, 26.26, 27.09, 28.59, 35.44, 35.50 (br), 38.21, 38.58, 39.52, 39.91, 51.38, 54.34, 77.94, 85.97, 126.94, 128.58, 129.45, 136.61, 142.70, 144.13, 144.30, 147.37, 162.80, 170.23. MS (ESI)  $m/z$  519.2 [ $\text{M} + \text{H}]^+$ . HRMS [ $\text{M} + \text{Na}]^+$  calcd, 541.2962; found, 541.2974.

**[(1R)-1-[(2S)-3-Phenyl-2-[(pyrazin-2-carbonyl)amino]-1-oxopropyl]amino]-3-methylbutyl]boronic Acid (MG341).** To the solution of **5d** (0.30 g, 0.58 mmol) and 2-methylpropylboronic acid (0.30 g, 1.68 mmol) dissolved in methanol (5 mL) and hexane (10 mL) was added 1 N HCl (1.5 mL). The reaction was stirred at room temperature for 18 h. The methanolic phase was washed with hexane ( $3 \times 10$  mL), and the hexane layer was extracted with methanol ( $3 \times 15$  mL). The combined methanolic layers were evaporated in vacuo, and the residue was dissolved in  $\text{CH}_2\text{Cl}_2$  (10 mL). The solution was washed with 5%  $\text{NaHCO}_3$  (10 mL), and the organic layer was dried over anhydrous  $\text{Na}_2\text{SO}_4$ , evaporated, and purified with chromatography ( $\text{CH}_3\text{OH}:\text{CHCl}_3 = 1:20$ ) to obtain 123 mg (56.4% yield) of a white foam solid. HPLC indicated a purity of 99.4 area%.  $^1\text{H}$  NMR ( $\text{CDCl}_3$ , 500 MHz)  $\delta$  0.69–0.80 ( $-\text{CH}_3$ , m, 3H), 1.11–1.15 ( $-\text{CH}$ , m, 1H), 1.23–1.25 ( $-\text{CH}_2$ , m, 2H), 1.79 ( $-\text{OH}$ , br s, 2H), 3.13–3.15 ( $-\text{CH}$ , m, 1H), 3.19–3.28 ( $-\text{CH}_2$ , m, 2H), 5.20 ( $-\text{CH}$ , q,  $J = 7.9$  Hz, 1H), 7.22–7.29 ( $-\text{Ph}$ , m, 5H), 7.38 ( $-\text{CONH}$ , br s, 1H), 8.29 ( $-\text{CONH}$ , d,  $J = 8.6$  Hz, 1H), 8.50 ( $-\text{Pyz}$ , m, 1H), 8.73 ( $-\text{Pyz}$ , d,  $J = 2.4$  Hz, 1H), 9.19 ( $-\text{Pyz}$ , d,  $J = 1.3$  Hz, 1H).  $^{13}\text{C}$  NMR ( $\text{CDCl}_3$ , 125 MHz)  $\delta$  22.16, 22.98, 25.35, 38.12, 39.66, 53.08, 127.11, 128.79, 129.45, 135.86, 142.72, 143.83, 144.36, 147.56, 162.90. MS (ESI)  $m/z$  407.2 [ $\text{M} + \text{Na}]^+$ . HRMS [ $\text{M} + \text{Na} + 2\text{CH}_2]^+$  calcd, 435.2189; found, 435.2147.

**[(1R)-1-[(2S)-3-Phenyl-2-[(1-naphthyl-2-carbonyl)amino]-1-oxopropyl]amino]-3-methylbutyl]boronic Acid (SMNT 1).** 34% yield, HPLC indicated a purity of 97.4 area%.  $^1\text{H}$  NMR ( $\text{CD}_3\text{OD}$ , 500 MHz)  $\delta$  0.83–0.96 ( $-\text{CH}_3$ , m, 6H), 1.22 ( $-\text{CH}$ , t,  $J = 7.4$  Hz, 1H), 1.41–1.43 ( $-\text{CH}_2$ , m, 2H), 2.73–2.78 ( $-\text{CH}$ , m, 1H), 3.10–3.21 ( $-\text{CH}_2$ , m, 2H), 5.12 ( $-\text{CH}$ , t,  $J = 8.1$  Hz, 1H), 7.30–7.32 ( $-\text{Ph}$ , m, 1H), 7.35–7.36 ( $-\text{Ph}$ , m, 4H), 7.43–7.53 ( $-\text{Ph}$ , m, 4H), 7.82–7.84 ( $-\text{Ph}$ , m, 1H), 7.88–7.91 ( $-\text{Ph}$ , m, 1H), 7.94–7.98 ( $-\text{Ph}$ , m, 1H).  $^{13}\text{C}$  NMR ( $\text{CD}_3\text{OD}$ , 125 MHz)  $\delta$  22.42, 23.74, 27.07, 38.40, 40.93, 52.97, 125.82, 126.35, 126.51, 127.46, 127.99, 128.28, 129.33, 129.79, 130.55, 131.34, 131.77, 135.12,

137.71, 172.39, 177.58. MS (ESI)  $m/z$  431.1 [ $\text{M} - \text{H}]^-$ , 455.2 [ $\text{M} + \text{Na}]^+$ . HRMS [ $\text{M} + \text{Na} + 2\text{CH}_2]^+$  calcd, 483.2431; found, 483.2436.

**[(1R)-1-[(2S)-3-(1-Naphthyl)-2-[(1-naphthyl-2-carbonyl)-amino]-1-oxopropyl]amino]-3-methylbutyl]boronic Acid (SMNT 2).** 52.5% yield, HPLC indicated a purity of 98.6 area%.  $^1\text{H}$  NMR ( $\text{CD}_3\text{OD}$ , 500 MHz)  $\delta$  0.61 ( $-\text{CH}_3$ , d,  $J = 6.6$  Hz, 3H), 0.80 ( $-\text{CH}_3$ , d,  $J = 6.5$  Hz, 3H), 1.02–1.11 ( $-\text{CH}_2$ , m, 2H), 1.23–1.25 ( $-\text{CH}$ , m, 1H), 2.00 ( $-\text{OH}$ , br s, 2H), 2.76 ( $-\text{CH}$ , q,  $J = 5.4$  Hz, 1H), 3.37–3.42 ( $-\text{CH}_2$ , m, 2H), 5.23 ( $-\text{CH}$ , t,  $J = 8.2$  Hz, 1H), 7.21–7.24 ( $-\text{Ph}$ , m, 1H), 7.44–7.49 ( $-\text{Ph}$ , m, 4H), 7.50–7.54 ( $-\text{Ph}$ , m, 2H), 7.79–7.83 ( $-\text{Ph}$ , m, 3H), 7.86–7.89 ( $-\text{Ph}$ , m, 3H), 7.94–7.96 ( $-\text{Ph}$ , m, 1H).  $^{13}\text{C}$  NMR ( $\text{CD}_3\text{OD}$ , 125 MHz)  $\delta$  21.92, 23.66, 26.66, 30.73, 38.77, 44.71, 53.18, 125.82, 126.18, 126.49, 126.98, 127.30, 127.40, 127.90, 128.41, 128.76, 128.90, 129.29, 129.54, 129.61, 131.72, 134.21, 134.73, 135.04, 172.40, 177.53. MS (ESI)  $m/z$  481.1 [ $\text{M} - \text{H}]^-$ , 505.2 [ $\text{M} + \text{Na}]^+$ . HRMS [ $\text{M} + \text{Na} + 2\text{CH}_2]^+$  calcd, 533.2587; found, 533.2291.

**[(1R)-1-[(2S)-3-(1-Naphthyl)-2-[(2-naphthyl-2-carbonyl)-amino]-1-oxopropyl]amino]-3-methylbutyl]boronic Acid (SMNT 3).** 68.3% yield, HPLC indicated a purity of 99.8 area%.  $^1\text{H}$  NMR ( $\text{CD}_3\text{OD}$ , 500 MHz)  $\delta$  0.52 ( $-\text{CH}_3$ , d,  $J = 6.5$  Hz, 3H), 0.74 ( $-\text{CH}_3$ , d,  $J = 6.5$  Hz, 3H), 0.90–0.98 ( $-\text{CH}_2$ , m, 2H), 1.00–1.06 ( $-\text{CH}$ , m, 1H), 2.00 ( $-\text{OH}$ , br s, 2H), 2.63 ( $-\text{CH}$ , q,  $J = 5.3$  Hz, 1H), 3.44 ( $-\text{CH}_2$ , dd,  $J_1 = 3.4$  Hz,  $J_2 = 8.7$  Hz, 1H), 5.13 ( $-\text{CH}$ , t,  $J = 7.8$  Hz, 1H), 7.44–7.49 ( $-\text{Ph}$ , m, 3H), 7.55–7.61 ( $-\text{Ph}$ , m, 2H), 7.80–7.85 ( $-\text{Ph}$ , m, 5H), 7.90–7.95 ( $-\text{Ph}$ , m, 3H), 8.34 ( $-\text{Ph}$ , s, 1H).  $^{13}\text{C}$  NMR ( $\text{CD}_3\text{OD}$ , 125 MHz)  $\delta$  21.84, 23.58, 26.54, 30.71, 38.71, 44.99, 53.46, 124.98, 126.91, 127.26, 127.93, 128.44, 128.71, 128.83, 129.03, 129.23, 129.37, 129.49, 130.05, 132.18, 133.99, 134.15, 134.70, 135.02, 170.45, 177.50. MS (ESI)  $m/z$  481.1 [ $\text{M} - \text{H}]^-$ , 505.2 [ $\text{M} + \text{Na}]^+$ . HRMS [ $\text{M} + \text{Na} + 2\text{CH}_2]^+$  calcd, 533.2587; found, 533.2786.

**Biological Testing.** The 20S proteasome activity assay kit was purchased from Chemicon (Chemicon, USA). Other reagents and solvents were purchased from commercial sources. In brief, substrates and compounds were previously dissolved in DMSO, with the final solvent concentration kept constant at 3% (v/v). The reaction buffers were (pH 7.5) 20 mM Tris, 1 mM DTT, 10% glycerol, and 0.02% (w/v) DS for CT-L activities. Proteasome activity was determined by monitoring the hydrolysis of the fluorogenic substrate, Suc-Leu-Leu-Val-Tyr-AMC ( $\lambda_{\text{exc}} = 360$  and  $\lambda_{\text{exc}} = 465$  nm for AMC substrates), reacting for 1 h at  $37^\circ\text{C}$  in the presence of untreated (control) or proteasome that had been incubated with different concentration of test compounds. Fluorescence was measured using an Infinite M200 microplate reader (Tecan, Austria).

#### ACKNOWLEDGMENT

This project was supported in part by Jiangsu Key Laboratory of Molecular Targeted Antitumor Drug Research Foundation (Grant BM2008201).

**Supporting Information Available:** General and experimental procedures, characterization data for **3a-d**, and output file of Catalyst run. This material is available free of charge via the Internet at <http://pubs.acs.org>.

## REFERENCES AND NOTES

- (1) Ciechanover, A. The ubiquitin-proteasome pathway: on protein death and cell life. *EMBO J.* **1998**, *17*, 7151–7160.
- (2) Rock, K. L.; Goldberg, A. L. Degradation of cell proteins and the generation of MHC class I-preserved peptides. *Annu. Rev. Immunol.* **1999**, *17*, 739–779.
- (3) Prösch, S.; Priemer, C.; Höflich, C.; Liebenthal, C.; Babel, N.; Krüger, D. H.; Volk, H. D. Proteasome inhibitors: a novel tool to suppress human cytomegalovirus replication and virus-induced immune modulation. *Antiviral Ther.* **2003**, *8*, 555–567.
- (4) Mitch, W. E.; Goldberg, A. L. Mechanisms of muscle wasting. The role of the ubiquitin-proteasome pathway. *New Engl. J. Med.* **1996**, *335*, 1897–1905.
- (5) Hampton, R. Y.; Gardner, R. G.; Rine, J. Role of 26S proteasome and HRD genes in the degradation of 3-hydroxy-3-methylglutaryl-CoA reductase, an integral endoplasmic reticulum membrane protein. *Mol. Biol. Cell* **1996**, *7*, 2029–2044.
- (6) Murakami, Y.; Matsufuji, S.; Kameji, T.; Hayashi, S.; Igarashi, K.; Tamura, T.; Tanaka, K.; Ichihara, A. Ornithine decarboxylase is degraded by the 26S proteasome without ubiquitination. *Nature* **1992**, *360*, 597–599.
- (7) Turner, G. C.; Du, F.; Varshavsky, A. Peptides accelerate their uptake by activating a ubiquitin-dependent proteolytic pathway. *Nature* **2000**, *405*, 579–583.
- (8) Naidoo, N.; Song, W.; Hunter-Ensor, M.; Sehgal, A. A role for the proteasome in the light response of the timeless clock protein. *Science* **1999**, *285*, 1737–1741.
- (9) Chain, D. G.; Schwartz, J. H.; Hegde, A. N. Ubiquitin-mediated proteolysis in learning and memory. *Mol. Neurobiol.* **1999**, *20*, 125–142.
- (10) Richardson, P. G.; Sonneveld, P.; Schuster, M. W.; Irwin, D.; Stadtmauer, E. A.; Facon, T.; Harousseau, J. L.; Ben-Yehu, D.; Lonial, S.; Goldschmidt, H. Bortezomib or high-dose dexamethasone for relapsed multiple myeloma. *New Engl. J. Med.* **2005**, *352*, 2487–2498.
- (11) Adams, J. Proteasome inhibition: a novel approach to cancer therapy. *Trends Mol. Med.* **2002**, *8* (Suppl.), S49–S54.
- (12) Adams, J.; Palombella, V. J.; Sausville, E. A.; Johnson, J.; Destree, A.; Lazarus, D. D.; Maas, J.; Pien, C. S.; Prakash, S.; Elliott, P. J. Proteasome inhibitors: a novel class of potent and effective antitumor agents. *Cancer Res.* **1999**, *59*, 2615–2622.
- (13) Pham, L.; Tamayo, A.; Lo, P.; Yoshimura, L.; Ford, R. J. Antitumor activity of the proteasome inhibitor PS-341 in mantle cell lymphoma B cells. *Blood* **2001**, *98*, 1945 (abstr 1945a, suppl).
- (14) Groll, M.; Berkers, C. R.; Ploegh, H. L.; Ovaa, H. Crystal structure of the boronic acid-based proteasome inhibitor bortezomib in complex with the yeast 20S proteasome. *Structure* **2006**, *14*, 451–456.
- (15) Adams, J.; Behnke, M.; Chen, S. W.; Cruickshank, A. A.; Dick, L. R.; Grenier, L.; Klunder, J. M.; Ma, Y. T.; Plamondon, L.; Stein, R. L. Potent and selective inhibitors of the proteasome: dipeptidyl boronic acids. *Bioorg. Med. Chem. Lett.* **1998**, *8*, 333–338.
- (16) Adams, J. Potential for proteasome inhibition in the treatment of cancer. *Drug Discov. Today* **2003**, *8*, 307–315.
- (17) Zhu, Y. Q.; Pei, J. F.; Liu, Z. M.; Lai, L. H.; Cui, J. R.; Li, R. T. 3D-QSAR studies on tripeptide aldehyde inhibitors of proteasome using CoMFA and CoMSIA methods. *Bioorg. Med. Chem.* **2006**, *14*, 1483–1496.
- (18) Zhu, Y. Q.; Lei, M.; Lu, A. J.; Zhao, X.; Yin, X. J.; Gao, Q. Z. 3D-QSAR studies of boron-containing dipeptides as proteasome inhibitors with CoMFA and CoMSIA methods. *Eur. J. Med. Chem.* **2009**, *44*, 1486–1499.
- (19) Zhu, Y. Q.; Zhao, X.; Zhu, X. R.; Wu, G.; Li, Y. J.; Ma, Y. H.; Yuan, Y. X.; Yang, J.; Hu, Y.; Ai, L.; Gao, Q. Z. Design, Synthesis, biological evaluation, and structure-activity relationship (SAR) discussion of dipeptidyl boronate proteasome inhibitors, Part I: comprehensive understanding of the SAR of  $\alpha$ -amino acid boronates. *J. Med. Chem.* **2009**, *52*, 4192–4199.
- (20) Catalyst, 4.11; Accelrys Inc.: San Diego, CA, USA.
- (21) Adams, J.; Ma, Y. T.; Stein, R.; Baevsky, M.; Grenier, L.; Plamondon, L. Boronic ester and acid compounds, synthesis and uses. *PCT Int. Appl.* **1995**, WO 1996013266.
- (22) Insight II, 2005; Accelrys Inc.: San Diego, CA, USA.
- (23) Johnsmael, J.; Byun, Y.; Jones, T. P.; Endo, Y.; Tjarks, W. A new strategy for molecular modeling and receptor-based design of carborane containing compounds. *J. Organomet. Chem.* **2003**, *680*, 223–231.
- (24) Johnsmael, J.; Byun, Y.; Jones, T. P.; Endo, Y.; Tjarks, W. A convenient method for the computer-aided molecular design of carborane containing compounds. *Bioorg. Med. Chem. Lett.* **2003**, *13*, 3213–3216.
- (25) Borissenko, L.; Groll, M. 20S proteasome and its inhibitors: crystallographic knowledge for drug development. *Chem. Rev.* **2007**, *107*, 687–717.
- (26) Klausner, Y. S.; Bodansky, M. Coupling reagents in peptide synthesis. *Synthesis* **1972**, 453–463.

CI900225S